ARTICLE IN PRESS

Available online at www.sciencedirect.com

SCIENCE DIRECT®

Aerosol Science III (III) III–III

Journal of Aerosol Science

www.elsevier.com/locate/jaerosci

High air flow, low pressure drop, bio-aerosol collector using a multi-slit virtual impactor

W. Bergman*, J. Shinn, R. Lochner, S. Sawyer, F. Milanovich, R. Mariella Jr.

Lawrence Livermore National Laboratory, Hazards Control Department, L379, P.O. Box 808, Livermore, CA 94551, USA

Received 16 May 2004; received in revised form 30 November 2004; accepted 22 December 2004

Abstract

A bio-aerosol collector was developed comprising a low pressure drop, multi-slit virtual impactor, a wetted wall cyclone collector from Research International (RI), and associated plumbing and blowers. The collector is portable, samples air at 1220 L/min, provides 3–8 mL liquid sample, and has 70 W power consumption. The RI collector was selected for this unit following an evaluation of leading commercial aerosol collectors. The compact, multi-slit virtual impactor has an area of 334 cm^2 and a pressure drop of 0.2 kPa at an inlet flow of 1220 L/min. The virtual impactor reported here concentrates the aerosols by a factor of four when the major to minor flow is adjusted to 4:1 ratio, but it has been field operated at a ratio of 8:1 when sampling at 2300 L/min. A preliminary evaluation of the RI-Lawrence Livermore National Laboratory collector was conducted to verify the unit has low pressure drop and can collect aerosols greater than 2 μm. A more detailed evaluation is needed to fully characterize the collector. This bio-aerosol collector has been incorporated in autonomous pathogen detection systems.
Published by Elsevier Ltd.

Keywords: Virtual impactor; Aerosol collector; Bio-aerosol

1. Introduction

Lawrence Livermore National Laboratory (LLNL) has been developing technology for the US government to address the threat of biological agents against civilian populations since 1996 (Milanovich, 1998). A key element of this program is the development of bio-detectors that can be used in the field by

* Corresponding author. Tel.: +1 925 422 5227; fax: +1 925 422 5176.
E-mail address: bergman2@llnl.gov (W. Bergman).

0021-8502/$ - see front matter Published by Elsevier Ltd.
doi:10.1016/j.jaerosci.2004.12.010

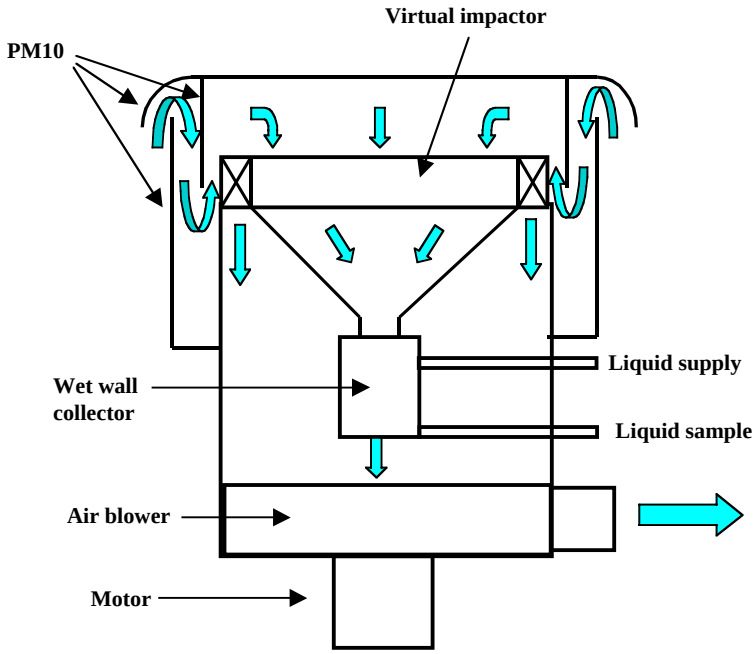

Fig. 1. Conceptual design of the commercially available XM2 aerosol collector that consists of a PM10 inlet to remove particles greater than 10 μm, a virtual impactor to concentrate the collected aerosols, and a wetted wall collector to trap the particles in a liquid.

emergency response personnel. Such a device would have to be portable and provide results in less than one hour. The leading technology for the detectors are a miniature flow cytometer that uses an immunoassay analysis to detect proteins on the surface of cells and a polymerase chain reaction (PCR) system to identify the DNA inside the cell (Milanovich, 1998). These analytical systems require a bio-aerosol collector that can rapidly collect sufficient airborne biological agents and inject them into a small water sample for subsequent analysis. A review of the common bio-aerosol collectors showed that a low power, portable, high sample volume collector with a small water sample was not available (Cox and Wathes, 1995; Macher and Burge, 2001; Reponen et al., 2001).

The reference bio-aerosol collector for biological warfare agents in the US is the XM2, which was developed in the early 1990s by the US military for use in the Biological Integrated Detection System (BIDS). The BIDS is a mobile biological laboratory used by the US Army since 1996 for sampling and analyzing for biological agents. An important component of the BIDS is the XM2 aerosol collector, that is used for obtaining aerosol samples for subsequent analysis. The XM2 collector consists of three stages illustrated in Fig. 1: a PM10 for removing particles larger than 10 μm, a virtual impactor for concentrating the aerosols, and a wetted wall collector for trapping the aerosols in a liquid. The particles suspended in the liquid, typically water, are analyzed in a subsequent analysis. The XM2 has been commercially available since the mid-1990s (SCP Dynamics, 7791 Elm St. NE, Minneapolis, MN 55432; Dycor, www.dycor.com) and is the conceptual design for the bio-aerosol collector in this study.

The objective of this study is to design and build a portable, low power consumption collector based largely on the XM2 design, except for the PM10 inlet, which was deferred to a future study. The desired

collector is smaller than 28 L ($0.03\,m^3$), injects the particles in a small liquid volume for subsequent analysis, and can function either as an independent unit or be coupled directly to a detector. To improve the collection rate of the collector, a multi-slit virtual impactor is developed and used as an aerosol concentrator at the inlet of the wet collector.

2. Evaluation of commercial collectors

Commercially available biological aerosol collectors are evaluated in this study to determine if they can be used in a high volume bio-aerosol collector. The collectors evaluated are the SASS 2000 unit (Research International, 17161 Beaton Road SE, Monroe, Washington 98272, www.resrchintl.com), SpinCon (Midwest Research Institute, 425 Volker Blvd, Kansas City, MO 64110, commercially available at Sceptor Industries, Inc., 4950 Cherry, Kansas City, MO 64110, www.sceptorindustries.com), SCAEP unit (Team Technologies, 90 Oak Street, Newton Upper Falls, MA 02164, www.epa.gov/boston/assistance/ceit_iti/tech_cos/tea.html), XM2 model SCP-1026 (SCP Dynamics, Inc., 7791 Elm St. NE, Minneapolis, MN 55432), and a glass impinger, model AGI-30 (Ace Glass, 1430 Northwest Blvd., Vineland, NJ 08362, www.aceglass.com). The XM2 collector is the current collector used in the US military, and the AGI-30 is a frequently used reference collector in comparative tests. Since SCP Dynamics is no longer in business, information on the XM2 collector can be obtained from Kesavan and Doherty (2001) and from another manufacturer (Dycor, 17944-106A Avenue, Edmonton, Alberta, Canada T5S 1V3, www.dycor.com). The XM2 model tested here (SCP-1026) uses a different design wet collector but is still based on turbulent wet scrubbing to remove particles.

The commercially available collectors are screened for aerosol removal efficiency using heterodisperse dioctyl sebacate (DOS) aerosols generated with a Laskin nozzle generator (Virtis, 815 Route 208, Gardiner, NY 12525) and an aerodynamic particle sizer (APS) (TSI, 500 Cardigan Road, Shoreview, MN 55126) to measure the aerosol size and concentration. Each of the collectors is connected to a source of constant aerosol concentration, and the aerosol concentration is measured at the inlet and the exhaust of the collector. Although this measurement determines the aerosol removal efficiency of the collector, it does not measure the collection efficiency in the liquid sample which takes into account particle loss in the collector. Thus, the screening tests using the aerosol samples represent an upper limit efficiency of the collectors assuming no internal particle loss. The collection efficiency in the liquid sample will be less due to aerosol losses such as deposition on the collector walls and particle residue in the wet collector.

The aerosol removal efficiency is determined from the aerosol concentration measurements in the inlet and exhaust of the collector using the following equation:

$$R = 100(1 - C_E/C_I) = E + L, \tag{1}$$

where R is the aerosol removal efficiency (%), E is the aerosol capture efficiency in the liquid sample (%), L is the aerosol loss in the collector (%), C_E is the aerosol concentration in the exhaust and C_I is the aerosol concentration in the inlet.

The results of the measurements are shown in Fig. 2, where the aerosol removal efficiency is plotted as a function of aerodynamic diameter. The aerosol removal efficiency of the collectors increases in the

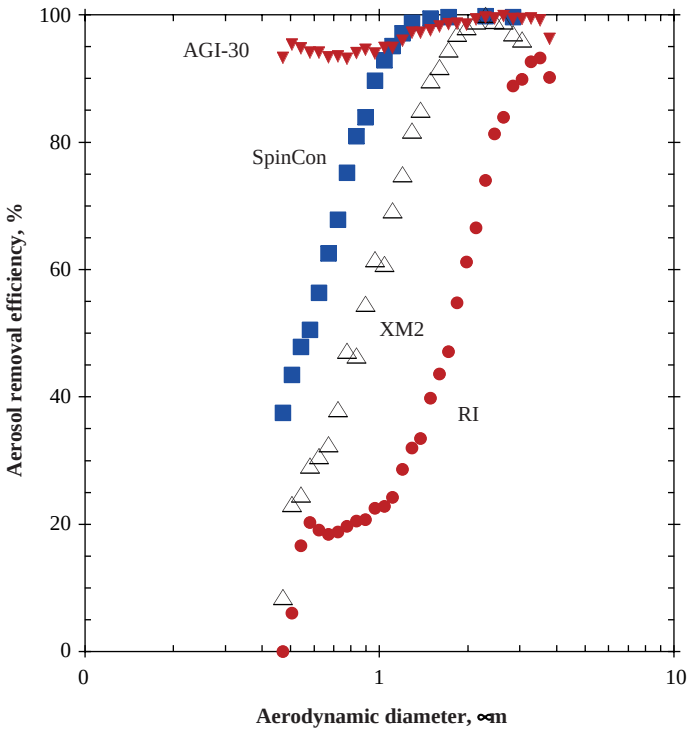

Fig. 2. Aerosol removal efficiency of commercially available aerosol collectors as a function of aerodynamic diameter. The removal efficiency is determined using DOS aerosols measured entering and exiting the collectors.

following sequence: AGI-30>SPINCON>XM2> Research International (RI). The aerosol removal efficiency for the SCAEP collector could not be determined because the exhaust contained too many aerosols that were generated in the electrostatic spraying process. However, because of additional problems such as periodic electrical shorts that shuts down the collector, high power consumption (220 W), and excessive size (57 L) and weight (20 kg), no attempt was made to obtain alternative efficiency measurements on the SCAEP collector.

The removal efficiency also varies with the type of aerosols sampled as seen in Fig. 3, where the aerosol removal efficiency of the RI collector is plotted as a function of aerodynamic diameter for DOS, AC Fine road dust (Powder Technology, Inc., 14331 Ewing Ave, South, Burnsville, MN 55337), and baker's yeast. Since the aerosol measurements are based on aerodynamic size, differences in density are already included in the size measurement. The road dust aerosol is generated using a TSI small-scale powder disperser, model 3433 and neutralized with a TSI Kr-85 neutralizer, model 3054. The higher removal efficiency for the road dust is probably due to the hygroscopic nature of the dust that causes an increase in particle size. The yeast aerosols are generated by creating a suspension of baker's yeast in water and nebulizing the suspension with a Wright nebulizer (Rabbe, 1976). The yeast aerosols have comparable efficiencies to the DOS aerosols, which are hydrophobic and do not adsorb much water. This follows because the yeast aerosols are saturated with water since they are freshly generated from a water suspension.

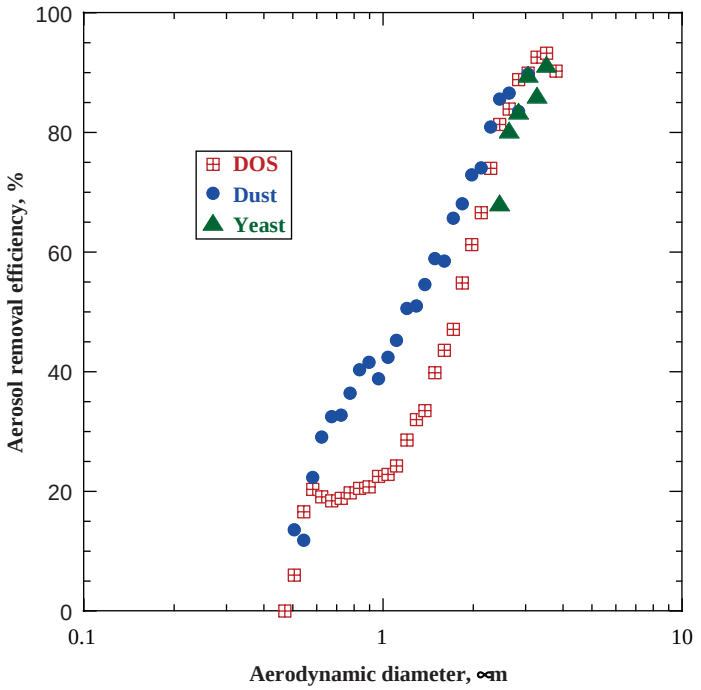

Fig. 3. Removal efficiency of DOS, road dust, and yeast for the RI collector as a function of the aerodynamic diameter.

The aerosol collection rate is a better measure of the various collectors than the removal efficiency because it provides a measure of the quantity of biological particles that are collected for subsequent analysis. The rate is determined by multiplying the removal efficiency by the sample flow rate. When this is done, the sequence of collectors arranged according to increasing aerosol removal rate is XM2>SpinCon>RI>AGI-30.

However, to evaluate the aerosol collectors for the application as a portable, low-power unit, the removal rates must be normalized to collector volume (or weight) and power consumption. The power consumption is computed from the current measurements using a clamp-on meter and the 110 V AC line voltage. The normalization is performed by dividing the collection rate by the collector volume or power consumption. Table 1 summarizes the values of key parameters of the collectors evaluated in this study. The AGI-30 collector has an external diaphragm pump included in the parameters for size, volume and weight. These parameter values are used to generate the collection rates normalized to collector volume and power consumption. The sequence of increasing removal rates when normalized for power consumption or volume is RI>XM2>SpinCon>AGI-30. The RI unit is the preferred collector from the commercial units tested here for integrating with the virtual impactor.

3. Determination of sample flow rate for RI-LLNL collector

The sample flow rate of the RI collector is too low to collect a sufficient concentration of aerosols in the liquid sample for the selected analytical techniques. The required air flow rate for the collector is

Table 1
Characteristics of commercially available collectors

Unit	Collector principle	Flow (L/min)	Weight (kg)	Volume (L)	Power (W)[a]
RI[b] Model SAAS2000	Impaction on wetted wall cyclone	265	3	14	13.8[c]
XM2 Model SCP-1026	PM10 virtual impaction to remove large particles, then concentration in two-stage virtual impactor, and then turbulent scrubbing in water reservoir	997	41	180	360
SCAEP Sentinel	Electrostatic capture by charged droplet scrubbing	360	20	57	220
SpinCon	Turbulent scrubbing and impaction on wetted wall cyclone	367	27	120	495
AGI-30[d]	Turbulent scrubbing in water reservoir	12	4	14	495

[a]All power measurements are made with line voltage.
[b]The liquid level is set to 8 mL.
[c]RI literature states 7.2 W when battery is used.
[d]A vacuum diaphragm pump is included with the AGI-30 to allow comparisons with the other collectors.

defined by

$$Q = \frac{C_D V_L F}{C_A (1 - L) t}, \tag{2}$$

where Q is the air flow rate (L/min), C_D the concentration detection limit in liquid (number agents/L), V_L the volume of liquid in collector (L), C_A the concentration of agents in air (number agents/L), t the air sample collection time (min), F the liquid sample dilution factor, greater or equal to 1, and L is the particle losses in the collector, fraction.

Eq. (2) shows that the flow rate is directly proportional to the volume of collected liquid and to the concentration detection limit of the analytical technique. Thus the smaller liquid volume and greater detector sensitivity (smaller C_D) favor smaller air sample flow rates.

The greatest factor affecting the required flow rate is the detection limit of the analysis method used. Belgrader et al. (1998) used immunoassay methods and found $C_D = 10^6$ cfu/L (colony forming units/liter) for the detection of bacterial spores of *Bacillis subtilis* var. *niger* (a simulant for anthrax) within 5 min. McBride et al. (2003) used immunoassay methods and found that C_D for *Bacillus anthracis* is 3×10^8 cfu/L and for *Yersinia pestis* is 6×10^6 cfu/L, both for a 1-min analysis. Belgrader et al. (1999) used PCR for nucleic-acid-based analysis of *Erwinia herbicola*, a vegetative bacterium. They found they could measure five bacteria in a 5 μL sample that was diluted with 20 μL of PCR mix. This corresponds to a concentration of 10^6 bacteria/L in the sample. Belgrader et al. (2003) also developed a flow-through PCR apparatus and showed they could detect less than three genomic DNA of *B. anthracis* (B.a.) in a 2 μL sample that was diluted with 9 μL PCR mix within 30 min. This corresponds to a concentration of 1.5×10^6 B.a./L. Thus the C_D values range from 10^6 to 3×10^8 for immunoassay analysis in 1–5 min and from 10^6 to 1.5×10^6 for PCR analysis in 7–30 min.

The other parameters in Eq. (2) have a much smaller effect on the required air flow. The most important of these is the liquid volume, where the required air flow is directly proportional to the liquid volume. The sample dilution factor takes into account any additional dilution of the sample by the reagents required in the sample preparation and analysis. For example if 20 μL of reagents are added to 5 μL of sample, then the dilution factor is 5. This parameter may be included in the detection limit or left as a separate parameter as in Eq. (2).

The particle loss term includes all losses that occur in the aerosol collection and in the liquid processing. In the tests using the RI collector, a significant fraction of the collected particles in the liquid sample remain as a residue in the wet wall cyclone. The test results are described later in this paper. It takes 2–3 collection cycles of clean sample to purge the residual particles from the RI collector. McBride et al. (2003) and Langlois et al. (2000) have observed these residual particles in their measurements and the subsequent purging with clean samples. The loss from additional components of the collector such as aerosol pre-treatment devices are also included in the loss term.

looseness=-1The volume flow rate needed for a bio-aerosol collector is estimated for applications where the collector is used to detect biological agents such as anthrax. Assuming $C_D = 3 \times 10^8$ cfu/L for immunoassay analysis of B.a., $V_L = 8$ mL, $F = 1$, and $L = 0.5$, then $Q = 4.8 \times 10^6 / C_A t$. For a 30-min sampling time per sample, the required flow rate is 160,000 L/min for $C_A = 1$ cfu/L and 1600 L/min for $C_A = 100$ cfu/L. If PCR is used for analyzing B.a., then C_D is 10^6 and $Q = 16,000 / C_A t$. Assuming a 30-min sampling time per sample, the required flow rate is 533 L/min for $C_A = 1$ cfu/L and 5.3 L/min for $C_A = 100$ cfu/L. It is clear that the much higher sensitivity of the PCR analysis will allow much lower sample flow rates.

Peters and Hartley (2002) have estimated that the lethal dose for 10% of people, LD(10), exposed to anthrax aerosols is 50–98 spores based on an extrapolation from studies of monkey exposures, where the lethal dose for 50% of the monkeys is 4100–8000 spores. Considering that normal human breathing is about 10 L/min, a 1-min exposure to a concentration of 10 cfu/L or a 10-min exposure to a concentration of 1 cfu/L can result in inhaling 100 spores. Although extrapolations from monkey exposure to human exposure to anthrax aerosols is tenuous, these extrapolations suggest that a bio-collector that proposes to detect bio-agents such as anthrax must have sample flow rates of several thousands of liters per minute using immunoassy methods and several hundreds of liters per minute using PCR methods.

Of the aerosol collectors evaluated in this study, only the XM2 at 997 L/min in Table 1 came close to meeting the flow requirement. To use the RI collector in a detection system for measuring exposures to anthrax and other bio-agents, the sample air flow has to increase from 265 L/min to at least 1600 L/min to allow detection of an average concentration of 100 cfu/L over a 30-min sampling period when using immunoassy detection methods. If a cloud of bio-agents is transient, then the peak concentration will have to be much higher than 100 cfu/L to provide a detectable measurement.

To develop a portable bio-aerosol collector, the concepts in the commercial XM2 collector shown in Fig. 1 are adopted whereby a PM-10 inlet removes particles larger than 10 μm, and two stages of virtual impactors are used to concentrate the ambient aerosols from about 1000 L/min to 20 L/min for collection in a wet collector (Kesavan and Doherty, 2001). The first stage virtual impactor in the XM2 consists of multiple opposing jets to concentrate the particles from an air flow of 1000 L/min to 100 L/min (Kesavan and Doherty, 2001). Marple and Liu (1987) and Marple et al. (1990) have developed the use of opposing jets for concentrating aerosols. A second stage virtual impactor, consisting of single opposing slits further concentrate the aerosols from 100 L/min to 20 L/min (Kesavan and Doherty, 2001).

Although the XM2 collector also has a PM10 inlet separator that consists of a tortuous path to reject particles larger than 10 μm, that component is not included in the RI-LLNL collector due to budget constraints. This important component will be added in the future.

4. Development of multi-slit virtual impactor

The virtual impactor to be used in the bio-aerosol sampler must have a low pressure drop in order to use a low power consumption blower. Marple and Liu (Marple and Liu, 1987; Marple et al., 1990) showed that multiple nozzles significantly reduce the pressure drop for a given flow rate and particle size cut point. They showed that the pressure drop is proportional to $n^{-2/3}$, where n is the number of nozzles. These findings are applicable for virtual impactors with round nozzles.

A similar derivation can be made for virtual impactors with rectangular nozzles following the same logic used by Marple et al. (1990) for virtual impactors with round nozzles. The basis for the derivation is that the Stokes number for virtual impactors for both round and rectangular nozzles remains relatively constant at the 50% cut point for a wide range of operating conditions. Thus the Stokes number (Stk) for a slit virtual impactor is given by (Marple et al., 2001)

$$Stk = \rho_p C_c d_p^2 U/(9\eta W) = \rho_p C_c d_p^2 Q/(9\eta W^2 Ln), \tag{3}$$

where ρ_p is the density of particle (g/cm^3), C_c the Cunningham slip correction factor (dimensionless), d_p the particle diameter (cm), U the average air velocity at the nozzle exit $= Q/nLW$ (cm/s), W the nozzle width (cm), L the nozzle length (cm), n the number of nozzles, and Q is the volumetric flow rate through the n nozzles (cm^3/s).

Since Stk is relatively constant at the 50% cut point, then assuming all of the parameters in Eq. (3) are constant except for W and n, we have

$$W^2 \propto 1/n. \tag{4}$$

From Bernoulli's equation, the pressure drop (ΔP) is proportional to the square of the average velocity in the nozzle,

$$\Delta P \propto U^2 = Q^2/(n^2 W^2 L^2). \tag{5}$$

Substituting the value of W^2 from Eq. (4) into Eq. (5) we have

$$\Delta P \propto 1/n. \tag{6}$$

Thus the pressure drop across a multi-slit virtual impactor is inversely proportional to the number of slits. The decrease in pressure drop with increasing number of slits for the slit virtual impactor ($1/n$) is greater than the corresponding decrease in pressure drop for a virtual impactor using circular nozzle ($1/n^{2/3}$). These relationships show the motivation for designing slit virtual impactors with many slits and small W. Romay, Roberts, Marple, Liu, and Oslon (2002) applied these principles by increasing the number of circular nozzles to decrease the pressure drop across the virtual impactor for developing an aerosol concentrator for biological agent detection. They developed a two-stage virtual impactor with 40 nozzles in the first stage to concentrate 300 L/min into 15 L/min output to the second stage. The second stage processed 15 L/min into 1 L/min output. Romay, Roberts, Marple, Liu, and Oslon (2002) experimentallymeasured the combined concentration increase for different particle sizes and ranged from 99 at 2.05 μm to 293 at 3.94 μm and 231 at 8.51 μm. These results show modest particle losses compared to the theoretical factor of 300 for no particle losses.

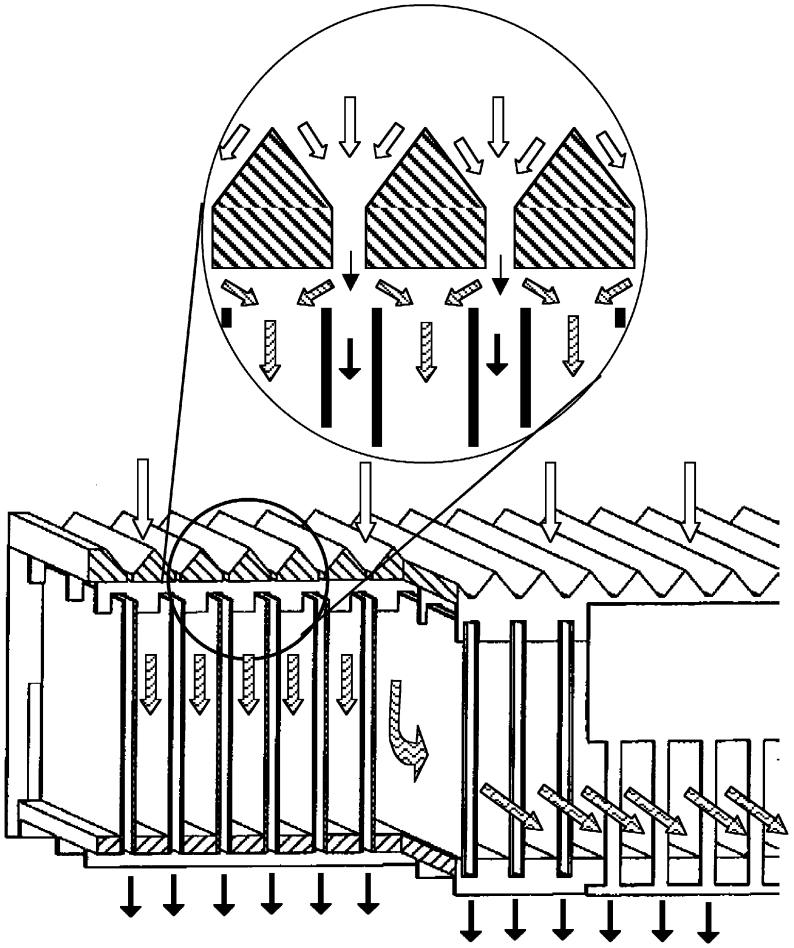

Fig. 4. Perspective drawing of the multi-slit, virtual impactor. The air in the accelerating slits forces particles into the collector slits due to particle inertia while the major air flow is deflected.

However, the pressure drop across the virtual impactor is 2.0 kPa for the first stage and 3.5 kPa for the second stage. These pressure drops are far too high for a low power consumption bio-collector. To achieve a pressure drop of less than 0.2 kPa at a flow of 1200 L/min, a virtual impactor with 186 nozzles is needed according to Marple's formula. However, such a design would not likely result in a low-cost virtual impactor because of the difficulty in aligning two sets of 186 nozzels.

To address this deficiency, a virtual impactor is developed based on a multi-slit design using the basic design criteria described by Marple and Chien (1980) and Marple et al. (2001) for cylindrical nozzle designs. Other researchers have previously developed single-slit virtual impactors (Sioutas, Koutrakis, & Burton, 1994). By having multiple slits with small channel width (0.5 mm), it is possible to achieve a very low pressure drop as indicated from Eq. (6). A perspective drawing of the multi-slit virtual impactor is shown in Fig. 4 , and the key design parameters are given in Table 2 (Bergman et al., 1999; Bergman, 2002).

Table 2
Design parameters for LLNL prototype multi-slit virtual impactor

Parameter	Value
Accelerator slit height	2.64 mm
Accelerator slit width	0.508 mm
Accelerator slit length	91.4 mm
Accelerator inlet funnel angle	45°
Collector slit height	22.1 mm
Collector slit width	0.762 mm
Collector slit length	91.4 mm
Accelerator to collector slit separation	1.52 mm
Slit to slit centers	4.24 mm
Number of slits per section	21
Number of sections per impactor	4

The particle laden air, shown as open arrows, enters from the top and is accelerated in the funnel section into the accelerator slits as shown in Fig. 4. Particles are forced into the collector slits due to their inertia and penetrate to the bottom of the impactor with the minor flow, shown as dark arrows. The major air flow, shown as shaded arrows, is deflected around the collector slits and into the more open exhaust channels. The major flow is pulled out at right angles through both ends of the virtual impactor. An end plate, partially shown in Fig. 4, covers the top portion of the major flow channels to promote the downward air flow prior to exiting the impactor as the major flow. The end plate also serves to seal the ends of the collector slits. Separation between the two plates defining each collector slit is maintained by dimples impressed on one of the plates.

Although there are no restrictions on the number of slits that can be used in a virtual impactor, there is a restriction on the length of the slits. Since most of the inlet air to the impactor is pulled out through the ends as the major flow, there is an increase in the inlet air velocity near both ends of the impactor. This uneven distribution of air velocity into the virtual impactor can be significant (increases with air flow and slit length) and is mitigated by restricting the length of the slits. The virtual impactor element in this report has a slit length of 9.14 cm and has 21 slits making the element approximately a square. Four vitual impactor elements are positioned in a square configuration with spaces between the adjacent elements that act as manifolds for the major air flow to be exhausted. The key features of the multi-slit virtual impactor are its small size relative to the air flow, the simplicity of its design and construction, and the very low pressure drop.

5. Integration of multi-slit virtual impactor with RI collector

Based on the evaluation of the commercial collectors, the RI collector was selected for use in the low power consumption, portable collector. A photograph of the RI collector (without the associated pumps, blower, controls, and housing) is shown in Fig. 5. Air enters at the bottom inlet into a cyclone at a 10° angle relative to the horizontal to force the air against the cyclone floor as well as against the circumferential surface. With 3–10 mL of water added to the base of the cyclone, the incoming air creates a swirling film of water on the exposed surfaces and forms a water curtain through which the inlet air passes. In

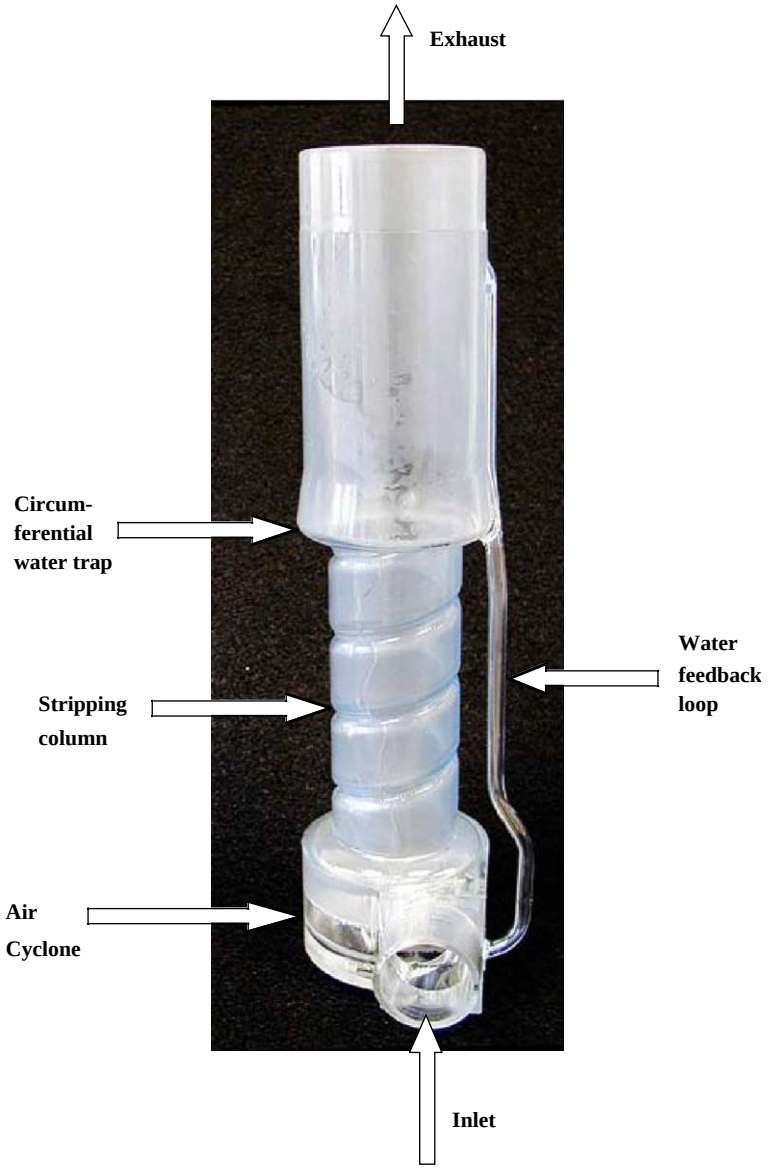

Fig. 5. Photograph of RI wetted-wall cyclone bioaerosol collector.

addition, a small nozzle in the center of the cyclone floor is used to generate a fine water spray. The highly turbulent and swirlingmixture of water droplets in the cyclone is effective in capturing small particles by impaction. These water droplets then strike the wall of the stripping column by centrifugal force. High air flow forces the collected water on the wall of the stripping column to flow into the circumferential water trap and then back into the air cyclone through the water feedback loop. The recycled water is forced through the spray nozzle at a flow rate of 30–100 cm^3/ min. Details of the operation are given in www.resrchintl.com.

Fig. 6. Photograph of assembled RI-LLNL collector with virtual impactor inlet showing.

RI built the integrated collector containing the multi-slit virtual impactor and the RI collector shown in Fig. 6. The unit is 43 cm × 25 cm × 34 cm. Sample air enters the virtual impactor from the top, and the minor flow exits from the bottom through a funnel and a tube to the inlet of the RI collector (not shown). The blower that is part of the RI collector is used to pull 265 L/min from the minor flow of the impactor through the RI collector. A separate blower is added to the integrated unit to remove the major flow of 955 L/min from the virtual impactor. Although the preferred design for the impactor exhaust is a manifold around the perimeter of the impactor with a connecting pipe to the exhaust blower, the alternative design shown in Fig. 6 was selected for expediency. The selected design consists of placing the virtual impactor and RI collector in a leak-free, sealing box and applying a vacuum to the box with the exhaust blower. The disadvantages of this approach are the added requirement of a leak-tight box and aerosol contamination of all the components within the box. These problems are eliminated in the next design, shown later, having an exhaust manifold around the perimeter of the virtual impactor. This design change does not impact the collector performance.

6. Evaluation of RI-LLNL collector

The performance of the RI-LLNL collector is determined using several different aerosols and different detection methods as illustrated in Fig. 7. The total inlet flow rate of 1220 L/min is measured directly with the Meriam laminar flow meter. The major flows from the virtual impactor (housing exhaust flow) and the exhaust flow from the RI collector are measured using hot wire anemometers placed in the respective exit pipes. The exhaust flow from the RI collector is also the minor flow from the multi-slit virtual impactor since the exit of the virtual impactor connects directly to the inlet of the RI collector. Converting the hot wire velocity measurements to flows yield 905 and 315 L/min for the exhaust and sample flows,

respectively. Thus, the virtual impactor reduces the sample flow to the RI collector to 315/1220 or 25% of the total flow; or, alternatively, the aerosol concentration is increased by a factor of 4. Pressure tap measurements in the tube leading from the virtual impactor to the RI collector show a pressure of 0.07 kPa. The pressure in the sealing box is 0.2 kPa. These measurements show that a flow of 1220 L/min into the virtual impactor splits into a sample flow of 315 L/min with a resistance of 0.07 kPa and an exhaust flow of 905 L/min with a resistance of 0.2 kPa. In alternative designs using a single blower, restrictions must be placed in the sample flow to equalize the pressure in both flows. The total power usage for the RI-LLNL collector is about 70 W, most of which is due to the blower pulling the major air flow from the virtual impactor.

A preliminary evaluation of the particle loss in the multi-slit virtual impactor is conducted using monodisperse DOS aerosols tagged with sodium fluorescene (SF) using the test apparatus shown in Fig. 7. The particle loss is determined by comparing the amount of tagged DOS aerosols entering the impactor and the amount of DOS aerosol trapped in the impactor. No measurements are made of the SF/DOS aerosols in the major or minor flows because special test fixtures for collecting the aerosols are not built into the impactor. Monodisperse particleshaving diameters of 5.1, 5.4, 7.4, and 14.7 μm are generated using various concentrations of DOS/SF in ethanol in a TSI vibrating orifice aerosol generator (VOAG), model 3450 (TSI, 500 Cardigan Road, Shoreview, MN 55126). The experiment illustrated in Fig. 7 consists of injecting DOS/SF aerosols into the top portion of the vertical test duct and thoroughly mixing with HEPA filtered air to produce 1220 L/min flow through the multi-slit virtual impactor. The impactor is mounted at the bottom of the rectangular duct and is sealed around the circumference of the impactor. A push–pull flow system is used to avoid creating a negative pressure at the collector inlet because of the resistance from the inlet HEPA filter and the Meriam laminar flow meter, model 50MC2-4 (Meriam Instrument, Cleveland, OH 44102). One blower upstream of the inlet HEPA filter provides the push, while a second blower downstream of the exhaust HEPA filter provides the pull.

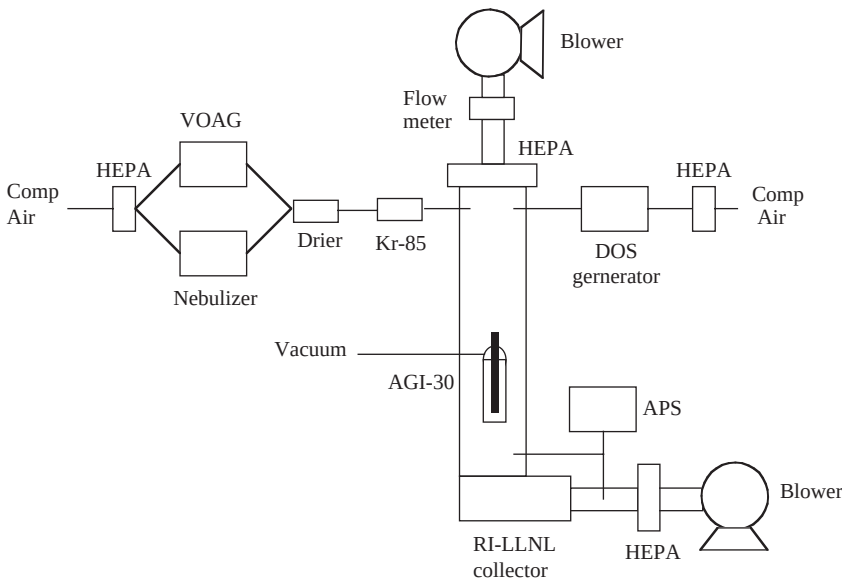

Fig. 7. Schematic of test apparatus used to evaluate RI-LLNL collector.

Table 3
Percent of aerosol lost in components of multi-slit virtual impactor

Component	Aerosol diameter (μm)			
	5.1	5.4	7.4	14.7
Accelerating slits (%)	2.6	9.9	3.4	17.7
Collector slits (%)	0.7	4.6	0.2	18.6
Bottom plate (%)	0.6	0.3	1.9	0.5
Total (%)	3.9	14.8	5.5	36.8

The impactor is operated for about 10 min, after which it is disassembled and rinsed with isopropyl alcohol to remove any DOS/SF deposits. The rinses from the top plate, the multiple plates defining the receiving slits, and the bottom plate are analyzed for SF and compared to the total SF entering the impactor. The rinses are adjusted to pH $\sim$ 9 to maximize the fluorescence and are analyzed with a spectrofluorometer, model FLUOROMAX2 (Horriba Jobin Yvon Inc., 3880 Park Avenue, Edison, NJ 08820). A series of calibration standards spanning several orders of magnitude were prepared to verify the rinse concentrations. The measured concentrations were in the linear range of the instrument response. To determine the total SF entering the virtual impactor, a HEPA filter paper is placed over the inlet of the impactor; and, following the exposure, the deposits are rinsed off. Separate tests are conducted for each aerosol size. No measurements are made after the virtual impactor using the DOS/SF aerosols to determine the separation efficiency of the impactor because a fixture for supporting a filter sample is not included in the collector design. In addition, no measurements are made of collected DOS/SF aerosols in the RI collector.

The rinses from the DOS/SF tests are analyzed and converted to percent of SF lost in the impactor for each of the impactor components and the total and are given in Table 3. Except for the 14.7 μm aerosol, the multi-slit virtual impactor typically has less than 15% particle loss. Because of the preliminary nature of this evaluation, the measurements are not repeated.

Aerosol removal efficiency tests for the RI-LLNL collector are conducted using heterodisperse DOS and 1.88 μm latex aerosols and the aerodynamic particle sizer (APS) as illustrated in Fig. 7. The heterodisperse DOS aerosols are generated using a Laskin nozzle generator (Virtis, 815 Route 208, Gardiner, NY 12525). The monodisperse latex aerosols are generated from a suspension using a Wright nebulizer (Rabbe, 1976) followed by a TSI drier and a TSI Kr-85 charge neutralizer. These tests provide the maximum potential collection efficiency if there are no losses in the collector or connecting tubing. The procedure is similar to that described in the section on evaluating commercial collectors. However, because there are one intake and two exhaust paths for the RI-LLNL collector (one from the virtual impactor exhaust and a second from the RI exhaust), separate measurements of the aerosol concentration and the flow rates of each of the three paths must be taken to compute the aerosol removal efficiency. The aerosol removal efficiency is determined from Eq. (7):

$$R = 100\{1 - [V_{RI}C_{RI} + V_{IE}C_{IE}]/[V_I C_I]\} = E + L, \tag{7}$$

where R is the aerosol removal efficiency (%), E the aerosol collection efficiency in liquid (%), L the aerosol loss in the collector (%), C the aerosol concentration, V the air flow rate, RI the measurement

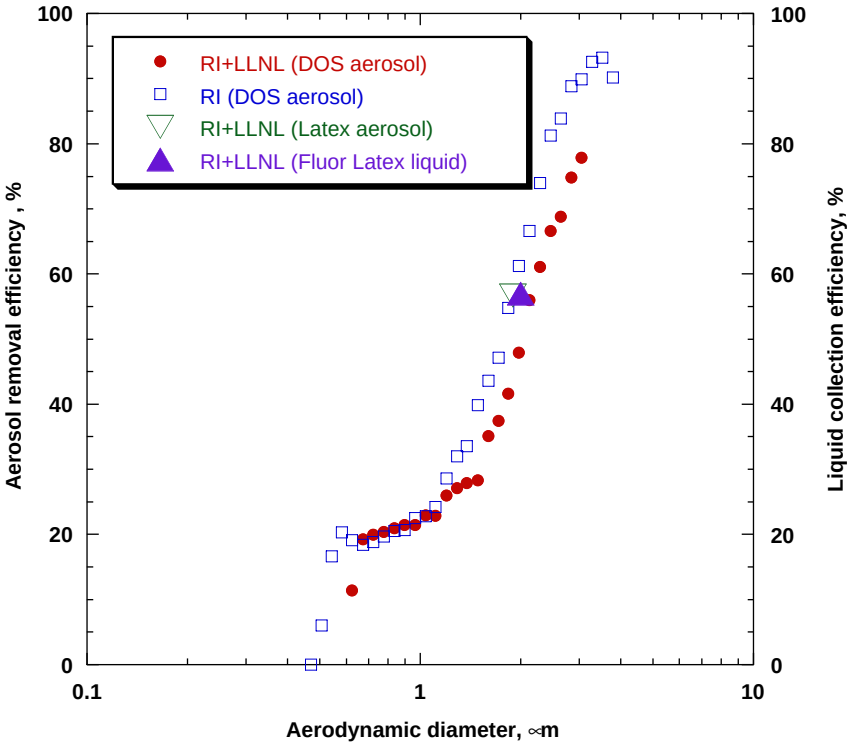

Fig. 8. Aerosol removal efficiency of RI and RI-LLNL collectors for DOS and latex aerosols and aerosol collection efficiency of RI-LLNL collector in liquid for fluorescent latex as a function of aerodynamic diameter.

at the exhaust of the RI unit, IE the measurement at the exhaust of the virtual impactor, and I is the measurement at the inlet of the virtual impactor.

Eq. (7) and the DOS and latex concentration measurements are used for determining the aerosol removal efficiency for the RI-LLNL collector. The results are shown in Fig. 8 along with the efficiency curve for the RI collector from Fig. 2.

In addition to the aerosol measurements, additional tests are conducted for measuring the collection efficiency in the liquid. The technique used for these tests is to use latex particles and a flow cytometer detector. In these tests, an AGI-30 collector is modified to have an isokinetic inlet probe directed vertical into the air stream. The modified AGI-30 collector is suspended inside the vertical duct to provide the measurement of the challenge aerosol in a liquid sample as is shown in Fig. 7. The AGI-30 is frequently used as a reference collector because of the nearly quantitative collection for particles greater than 0.5 μm as seen in Fig. 2. The particle collection efficiency in this test is determined from the fraction of particles collected in the RI-LLNL liquid sample to the particles collected in the AGI-30, both measurements corrected for the corresponding sample flow rates. Since the AGI-30 only samples 12 L/min compared to the 1220 L/min for the RI-LLNL collector, the number of particles in the AGI-30 are multiplied by 100 for the comparison.

Green fluorescent 2.0 μm latex aerosols (Duke Scientific, 2463 Farber Place, Palo Alto, CA 94303, www.dukesci.com) are used in these tests, and the particle concentration is measured in the AGI-30 and

RI-LLNL liquid samples using a flow cytometer (Mariella Jr., Huang, & Langlois, 1999). The fluorescent latex aerosols are generated in a water suspension using the Wright nebulizer in Fig. 7. The fluorescent latex is used because non-fluorescent latex cannot be distinguished from background debris in the AGI-30 sample. These liquid measurements show the total collection efficiency of the RI-LLNL collector with three rinses is 57% for the fluorescent 2.0 μm latex aerosols. For 2.0 μm particles, the liquid collection efficiency is in good agreement with the aerosol removal efficiency as seen in Fig. 8. However, no other latex sizes are tested here because of time limitations in the collector development. More extensive tests are planned for the future.

An important finding of the liquid particle measurements is the residue of particles remaining in the RI-LLNL collector. After removing the 3 mL sample, fresh water is added and the unit operated for about 5 min. This second sample is removed and a third charge of fresh water is added and operated for 5 min. Each of the three samples are analyzed for latex particles. The analysis shows that the first three samples contain 64.5%, 33% and 2.5% of the total particles counted. The observations are made while measuring the collection efficiency of the fluorescent PSL spheres in the RI-LLNL collector. No attempt was made to study this phenomenon in detail but only to report the observation. Thus there is considerable residue of particles in the RI collector and should be considered when correcting for particle loss and for cross-contamination of sequential samples. In practice, the residue does not pose a problem for cross contamination of sequential samples since the collector is designed as a detect-to-treat instrument. Once there is a positive sample, the subsequent samples only serve to confirm the reading.

Fig. 8 shows that the DOS aerosol removal efficiency for the RI-LLNL collector is only slightly lower than the comparable removal efficiency for the RI collector alone. Although the RI-LLNL collector uses only 3 mL of water in the wetted cyclone compared to 8 mL in the RI collector test, the lower efficiency is believed to be primarily due to the aerosol losses in the virtual impactor and associated tubing. The aerosol test on the RI-LLNL collector using 1.88 μm latex shows a removal efficiency of 57%, which is comparable to the DOS removal efficiency measurements on the RI collector but is 12% higher than the DOS efficiency measurements on the RI-LLNL collector. It is possible that particle bounce for the solid latex aerosols will result in less particle loss in the impactor than for the DOS aerosol and thus will have a higher removal efficiency in the RI-LLNL collector. However, small differences in the efficiency measurements (i.e. ±5%) are generally due to experimental variability.

Another finding seen in Fig. 8 is that the collection efficiency determined from the fluorescent latex particles collected in the liquid sample is comparable to the aerosol removal efficiency determined from DOS aerosol samples. The RI-LLNL collection efficiency of latex spheres in the liquid sample is 57% compared to 50% for the removal efficiency of DOS aerosols in the air sample. The 57% efficiency represents the total number of spheres measured in the sample plus the residues from two additional rinses. For comparison, the RI collector has an aerosol removal efficiency of 62% for DOS aerosols. Since the variability of the efficiency measurements is estimated at ±5%, these measurements are not significantly different.

Since the rate of aerosol collection is the critical parameter in evaluating collector performance, the removal efficiency measurements in Fig. 8 are converted to the collection rate by multiplying the removal efficiencies in Fig. 8 by the corresponding sample flow rates and the aerosol concentration (assumed 1 particle/L). The results show that the aerosol collection rate of the RI-LLNL collector is about four times that of the RI collector alone. This increased collection rate is due to the virtual impactor, that effectively concentrates the larger aerosols into a smaller air flow.

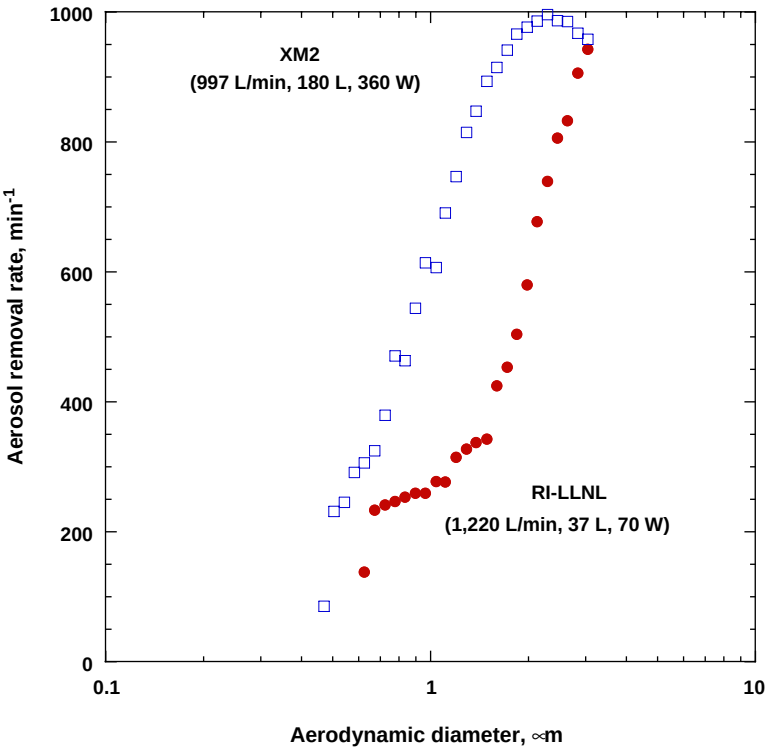

Fig. 9. Comparison of DOS aerosol removal rates of the RI-LLNL collector to the XM2 collector as a function of aerodynamic diameter. Collector flow rate, size and power consumption are shown in parentheses.

To assess the performance of the RI-LLNL collector relative to the XM2 collector, which is the current reference collector in the US, the collection rates of the two collectors are plotted in Fig. 9. This figure shows that the XM2 has a significantly higher collection rate for aerosols below 3 μm. Above 3 μm, the two collectors have similar collection rates. However, the XM2 is much larger and requires much more power than the RI-LNL collector. In summary, the portability and the low power consumption of the RI-LLNL collector more than compensate for the lower collection rate at the smaller aerosol sizes.

Since the bio-aerosol collector described in this report was first completed in 1999 (Bergman et al., 1999), the unit has been repackaged into a smaller size (approximately a 30 cm cube) as shown in Fig. 10. A manifold is also added to the virtual impactor to exhaust the major flow through a tube rather than in an evacuated chamber. This modification, which is the original design based on the XM2, prevents ambient aerosols from contaminating the interior of the collector components. A more powerful blower is added to the collector to increase the sample flow rate to 2300 L/min (McBride et al., 2003). A rain cap is also added to the inlet of the virtual impactor to prevent rain and large objects (but not large particles) from being pulled into the collector. The improved collector has been evaluated in field tests (Langlois et al., 2000; McBride et al., 2003) and a number of units have been built and deployed in limited applications for monitoring for bio-agents. When the PM10 inlet for removing particles larger than 10 μm is added in the future, the portable collector will have all of the major design concepts from the XM2 shown in Fig. 1.

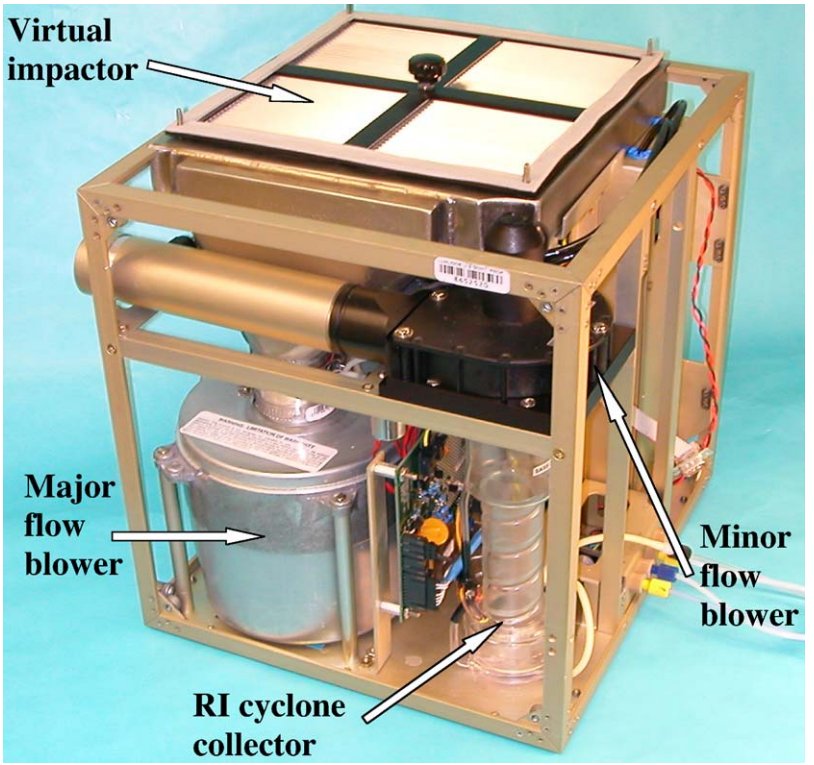

Fig. 10. Photograph of the repackaged RI-LLNL collector showing the virtual impactor, the major flow and minor flow blowers, and the RI collector.

7. Summary and conclusions

A high flow rate, low pressure drop bio-aerosol collector is developed that is portable and has low-power consumption. The collector design is based on the commercially available XM2 collector, which is the standard collector for biological warfare agents in the US. The collector described in this report samples air at 1220 L/min and has a flow resistance of 0.2 kPa. The bio-aerosol collector consists of a multi-slit virtual impactor, a wetted-wall cyclone collector from RI, two blowers and associated plumbing and controls.

The RI collector was selected from an evaluation of leading commercial collectors based on high sample volume (365 L/min), low-power consumption (13.8 W), and small volume of collected water (3–8 mL). Efficiency tests using DOS aerosols show an increasing aerosol removal efficiency with particle size from 22% at 1.0 μm to 50% at 1.75 μm and to 90% at 3.0 μm. Other aerosols such as latex spheres and yeast cells show comparable efficiencies, while Arizona road dust has higher efficiency presumably due to water adsorption.

The multi-slit virtual impactor consists of four modules, 9.1 cm^2 and 2.5 cm thick packaged into a 23 cm^2 and 2.5 cm thick unit. Each of the modules have 21 virtual impactor slits that are 4.24 mm apart. The effective open area of the virtual impactor is 11.8%, which represents the relative area of the accelerating slits compared to the total area. The high density of the slits is responsible for the

low flow resistance of the multi-slit virtual impactor. At 1220 L/min flow, the pressure drop across the virtual impactor is 0.2 kPa. Preliminary tests using fluorescent DOS aerosols show that there is less than 15% particle loss in the virtual impactor between 5 and 7 μm. More extensive tests are planned to fully characterize the virtual impactor performance.

The RI wet wall cyclone and the multi-slit virtual impactor are integrated to create the RI-LLNL collector, in which the minor flow from the virtual impactor enters the RI collector. The RI-LLNL collector samples 1220 L/min and has a power consumption of about 70 W. Aerosol removal efficiency measurements are made using DOS aerosols and latex spheres by measuring the aerosol concentration entering the exiting collector. The removal efficiency with DOS aerosols is 22% at 1.0 μm, 50% at 2.0 μm, and 77% at 3.0 μm diameter. These collection efficiencies are slightly less than that for the RI unit alone because of particle loss in the virtual impactor. The particle removal efficiency using 1.88 μm diameter latex spheres in aerosol measurements is 57%. A separate test using fluorescent latex spheres and measuring the quantity of spheres in the liquid sample show the collection efficiency for 2 μm spheres is 57%. The liquid sample confirms that the efficiency measurements with aerosols are an approximate assessment of the collector efficiency.

The collector described in this report has been repackaged into a smaller size and incorporated into autonomous pathogen detection systems (Langlois et al., 2000; McBride et al., 2003). These detection systems are large units, about the size of an automated teller machine and are not portable. Future efforts are aimed at reducing the size and portability of these pathogen detection systems, including the aerosol collector described here.

Acknowledgements

The authors thank Dr. James M. Clark and two anonymous reviewers for many helpful comments and suggestions in preparing this paper. This work was performed under the auspices of the US Department of Energy by University of California, Lawrence Livermore National Laboratory, under Contract W-7405-Eng-48.

References

Belgrader, P., Bennett, W., Bergman, W., Langlois, R., Mariella, R., Jr., Milanovich, F., Miles, R., Venkateswaran, K., Long, G., & Nelson, W. (1998). Autonomous system for pathogen detection and identification. *SPIE Proceedings, 3533*, 198–206.

Belgrader, P., Benett, W., Hadley, D., Richards, J., Stratton, P., Mariella, R., Jr., & Milanovich, F. (1999). PCR detection of bacteria in seven minutes. *Science*, *284*(5413), 449–450.

Belgrader, P., Elkin, C. J., Brown, S. B., Nasarabadi, S. N., Langlois, R. G., Milanovich, F. P., & Colston, B. W., Jr. (2003). A reusable flow-through polymerase chain reaction instrument for the continuous monitoring of infectious biological agents. *Analytical Chemistry*, *75*, 3446–3450.

Bergman, W. (2002). Low pressure drop, multi-slit virtual impactor. United States Patent, US 6,402,817 B1.

Bergman, W., Shinn, J., Lochner, R., & Sawyer, S. (1999). *RI-LLNL hybrid biological aerosol collector*. Lawrence Livermore National Laboratory, UCRL-ID-35282, http://www.llnl.gov/library/.

Cox, C. S., & Wathes, C. M. (1995). *Bioaerosols handbook*. Boca Raton, FL: Lewis Publishers.

Kesavan, J., & Doherty, R. W. (2001). *Characterization of the SCP 1021 Aerosol Sampler*. Edgewood Chemical Biological Center Report ECBC-TR-211, Aberdeen Proving Ground, MD. Available from National Technical Information Service, 5285 Port Royal Road, Springfield, VA 22161, report ADA397460, www.ntis.gov.

Langlois, R. G., Brown, S., Colston, B., Jones, L., Masquelier, D., Meyer, P., McBride, M., Nasarabadi, S., Ramponi, A. J., Venkateswaran, K., & Milanovich, F. (2000). Development of an autonomous pathogen detection system. In *Proceedings of the first joint conference on point detection*, Wlliamsberg, VA, October 23–27, 2000. http://www.llnl.gov/tid/lof/documents/pdf/238720.pdf.

Macher, J. M., & Burge, H. A. (2001). Sampling biological aerosols. In B. S. Cohen, & C. S. McCammon Jr. (Eds.), *Air sampling instrument* (9th ed., pp. 661–701). American Conference of Governmental Industrial Hygienists, Cincinnati, www.acgih.org/store.

Mariella, R. P., Jr., Huang, Z., & Langlois, R. G. (1999). Characterization of the sensitivity of side scatter in a flow-stream waveguide flow cytometer. *Cytometry*, *37*, 160–163.

Marple, V. A., & Chien, C. M. (1980). Virtual impactors: a theoretical study. *Environmental Science and Technology*, *14*, 975–985.

Marple, V. A., & Liu, B. Y. H. (1987). High volume virtual impactor. United States Patent, US 4,670,135.

Marple, V. A., Liu, B. Y. H., & Burton, R. M. (1990). High-volume impactor for sampling fine and coarse particles. *Journal of Air and Waste Management Association*, *40*, 762–767.

Marple, V. A., Olson, B. A., & Rubow, K. L. (2001). Inertial, gravitational, centrifugal, and thermal collection techniques. In P. A. Baron, & K. Willeke (Eds.), *Aerosol measurement, principles, techniques, and applications* (2nd ed.). New York: Wiley-Interscience (pp. 229–260).

Milanovich, F. (1998). *Reducing the threat of biological weapons*. LLNL's Science & Technology Review, Lawrence Livermore National Laboratory, June, http://www.llnl.gov/str/Milan.html.

McBride, M. T., Masquelier, D., Hindson, B. J., Makarewicz, A. J., Brown, S., Burris, K., Metz, T., Langlois, R. G., Tsang, K. W., Byron, R., Anderson, D. A., Venkateswaran, K. S., Milanovich, F. P., & Colston, B. W., Jr. (2003). Autonomous detection of aerosolized *Bacillus anthracis* and *Yersinia pestis*. *Analytical Chemistry*, *75*, 5293–5299.

Peters, C. J., & Hartley, D. M. (2002). Anthrax inhalation and lethal human infection. *Lancet*, *359*, 710.

Rabbe, O. G. (1976). The generation of aerosols of fine particles. In B. Y. H. Liu (Ed.), *Fine particles, aerosol generation, measurement, sampling, and analysis*. New York: Academic Press, Inc. (pp. 57–110).

Reponen, T., Willeke, K., & Grinshpun, S. (2001). Biological particle sampling. In P. A. Baron, & K. Willeke (Eds.), *Aerosol measurement, principles, techniques, and applications* (2nd ed.). New York: Wiley-Interscience (pp. 751–777).

Romay, F. J., Roberts, D. L., Marple, V. A., Liu, B. Y. H., & Oslon, B. A. (2002). A high-performance aerosol concentrator for biological agent detection. *Aerosol Science and Technology*, *36*, 217–226.

Sioutas, C., Koutrakis, P., & Burton, R. M. (1994). Development of a low cutpoint slit virtual impactor for sampling ambient fine aerosols. *Journal of Aerosol Science*, *24*, 1321–1330.